Cosmic Masers - from OH to H_0
Proceedings IAU Symposium No. 287, 2012
R.S. Booth, E.M.L. Humphreys & W.H.T. Vlemmings, eds.

doi:10.1017/S1743921312006679

The magnetic field of IRAS 16293-2422 as traced by shock-induced H_2O masers

Felipe O. Alves[1], **Wouter H. T. Vlemmings**[2], **Josep M. Girart**[3] and **José M. Torrelles**[4]

[1]Argelander-Institut für Astronomie, University of Bonn,
Auf dem Hügel 71, D-53121, Bonn, Germany
email: falves@astro.uni-bonn.de

[2]Chalmers University of Technology, Onsala Space Observatory,
SE-439 92 Onsala, Sweden
email: vlemmings@chalmers.se

[3]Institut de Ciències de l'Espai (IEEC-CSIC), Campus UAB, Facultat de Ciències,
C5 par 2ª, 08193 Bellaterra, Catalunya, Spain
email: girart@ice.cat

[4]Institut de Ciències de l'Espai (CSIC)-UB/IEEC, Universitat de Barcelona,
Martí i Franquès 1, E-08028 Barcelona, Spain
email: torrelles@ieec.cat

Abstract. H_2O masers are important magnetic field tracers in very high density gas. We show one of the first magnetic field determinations at such high density in a low-mass protostar: IRAS 16293-2422. We used the Very Large Array (VLA) to carry out spectro-polarimetric observations of the 22 GHz Zeeman emission of H_2O masers. A blend of at least three maser features can be inferred from our data. They are excited in zones of compressed gas produced by shocks between the outflows ejected by this source and the ambient gas. The post-shock particle density is in the range 1 - 3 $\times 10^9$ cm^{-3}, and the line-of-sight component of the magnetic field is estimated as $\sim$ 113 mG. The outflow dynamics is likely magnetically dominated.

Keywords. stars: formation, masers, polarization, ISM: magnetic fields, ISM: individual: IRAS 16293-2422

---

1. Introduction

Water masers are unique because they are found in a variey of astrophysical environments, including star-forming regions at distinct mass ranges. The most commonly observed water maser line is the ($6_{16} - 5_{23}$) transition at 22 GHz, an excellent probe of molecular gas at very high volume densities ($n \sim 10^{8-10}$ cm^{-3}, Elitzur *et al.* 1989). Spectro-polarimetry of water masers is a powerful tool to study magnetic fields at such high densities, since the strength of the maser line emission is such that the small splitting due to the Zeeman effect can be detected. This allows the line-of-sight (LOS) component of the magnetic field to be determined. If the linear polarization is also measured, then the full 3D magnetic field configuration can be derived.

Very Long Baseline Interferometry (VLBI) of water masers reveals the magnetic field properties at very small (subarcseconds) spatial scales, resolving its structure in the dense molecular material around circumstellar envelopes of young stars (Vlemmings *et al.* 2006). Moreover, this technique overcomes the depolarization issue, when a decrease in the polarization degree is observed toward high extinction media due to unresolved fields or roundness of dust grains (Goodman *et al.* 1995, Lazarian *et al.* 1997). Therefore, multi-wavelength polarimetry allows for tracking the magnetic field morphology from the

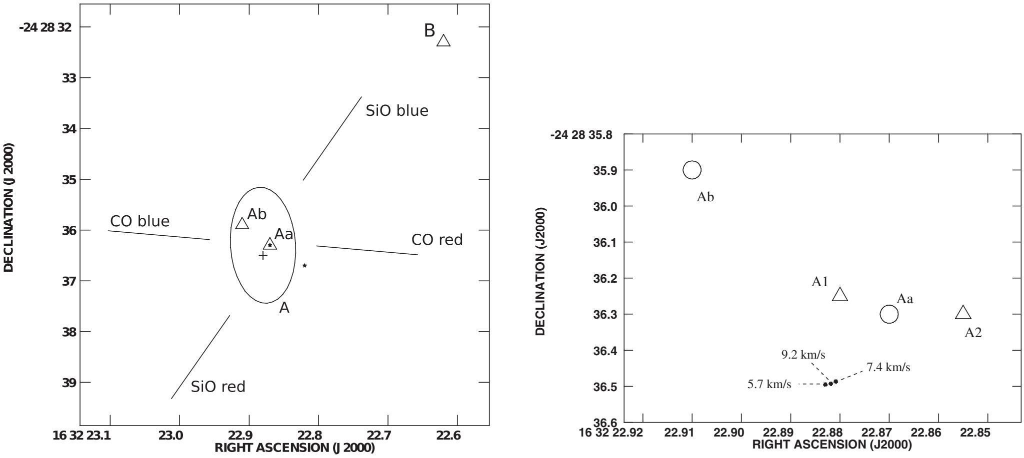

Figure 1. *Left panel*: Distribution of dust and molecular material in I16293. The plus signal indicates the position of our VLA water maser data. The ellipse is the deconvolved size of the source *A* as derived by Rao *et al.* (2009). Triangles denote the position of the submm condensations observed by Chandler *et al.* (2005). Stars denote the VLBI water maser detections of Imai *et al.* (2007) and straight lines denote the direction of the quadrupolar outflow. *Right panel*: Possible independent maser features (stars) as derived by our gaussian fit. The numeric labels are the maser velocities with respect to the Local Standard of Rest (LSR). The 3.7 cm sources *A1* and *A2* (triangles) and the submm sources *Aa* and *Ab* (circles) are also shown (Chandler *et al.* 2005).

diffuse gas of molecular clouds to dense cores. In this case, the magnetic field strength is expected to increase as a function of the volume density, as observationally shown by Fiebig & Guesten (1989).

In this work, we report spectro-polarimetric Very Large Array (VLA) observations of H_2O masers toward IRAS 16293-2422 (hereafter, I16293). This object is a well studied Class 0 low-mass binary protostar (separation $\sim$ 600 AU), with a very rich chemistry (Jørgensen *et al.* 2011). The brightest component (source *A*) has a very strong submillimeter (submm) flux and is resolved into two condensations: *Aa* and *Ab* (Chandler *et al.* 2005). A quadrupolar outflow configuration is also observed in SiO and CO molecular emission.

H_2O maser emission in I16293 has been well monitored and shows strong (> 200 Jy) and stable emission over a few weeks but highly variable over months (Claussen *et al.* 1996, Furuya *et al.* 2003). The observed features are detected only toward source *A* and have proper motions of $\sim$ 5.6 mas/yr (Imai *et al.* 2007). The maser spots are mainly associated with the outflows around the source and its circumstellar disk.

2. Observations and Results

The observations were performed with the VLA in extended A-configuration, on 2007 June 25th and 27th. Each track lasted $\sim$ 5.5 hours. A total of 27 antennas were used, 10 of them already retroffited with the new system, resulting in a combined VLA/EVLA (Extended VLA) observation. We used the K band receivers tuned at the frequency of the water maser ($6_{16} - 5_{23}$) rotational transition ($\mu_0 = 22.23508$ GHz), and the full polarization capability of the correlator. The spectral setup is 10.5 km s^{-1} wide, with a spectral resolution of 0.08 km s^{-1}, and it covers the brightest maser features observed around 7 km s^{-1}. Data reduction was done with the Astronomical Image Processing

https://doi.org/10.1017/S1743921312006679 Published online by Cambridge University Press

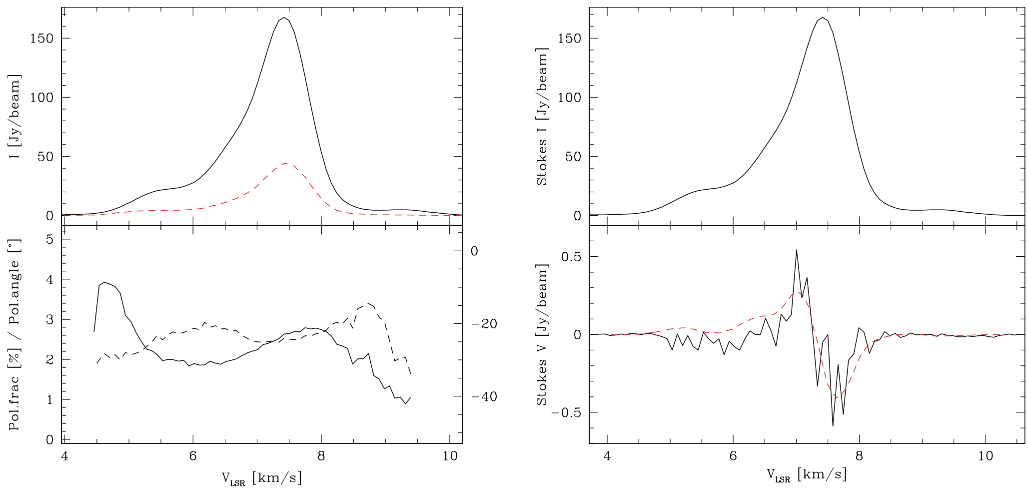

Figure 2. *Left panel*: Stokes I (black line) and linear polarization intensity (multiplied by a factor of 10, red dashed line) spectra of water maser emission (upper panel). The spectra of polarization fraction (black line, left scale) and position angle (dashed line, right scale) are also shown (lower panel). *Right panel*: Stokes I (upper panel) and Stokes V (lower panel) spectra of the water maser emission. The red dashed line is the scaled derivative of total power I.

Table 1. H_2O maser components in IRAS 16294-2422.

V_{LSR} (km s^{-1})	I^{a}_{peak} (Jy $beam^{-1}$)	α (2000) (h m s)	δ (2000) (o ′ ″)
5.7	23	16 32 22.8830	−24 28 36.495
7.4	168	16 32 22.8808	−24 28 36.487
9.2	5	16 32 22.8818	−24 28 36.493

Notes: [a] Equatorial coordinates derived with the JMFIT task of AIPS.

Software package (AIPS). Imaging of Stokes parameters I, Q and U were generated with a quasi-uniform weighting. The resulting synthesized beam is $0.14'' \times 0.08''$.

The water masers detected in our observations are associated with source *A* with a projected distance of $\sim$ 30 AU from the dust condensation *Aa* (Fig. 1, left panel). The maser line peaks at 7.4 km s^{-1} with a flux density of 170 Jy $beam^{-1}$ and a rms noise of 8 mJy $beam^{-1}$ and 23 mJy $beam^{-1}$ for edge channels and channels containing emission, respectively. The Stokes I spectrum has a non-Gaussian line profile, and at least three unresolved components can be inferred from the spectrum (Fig. 2, upper panels). A two-dimensional Gaussian profile fit on those components provides a mean spatial separation of 22 milliarcseconds. The equatorial coordinates and the peak intensity of each component is shown in Table 1. The three features are linearly distributed in a E-W direction (Fig. 1, right panel) and have the same LSR velocity as the SE outflow lobes (Rao *et al.* 2009). In addition to the submm sources, two centimeter (cm) sources (*A1* and *A2*) were observed in the same region and might be associated with a radio jet and to a protostar (Chandler *et al.* 2005). This reinforces that our maser features are excited by shocks in the dense gas at the surroundings of condensation *Aa*.

Polarized emission: The spectrum of linearly polarized intensity is very similar to the Stokes I line profile except for the flux scale, which is weaker by a factor of $\sim$ 30. (Fig. 2, left-upper panel). The measured polarization fraction is $2.5 \pm 0.2\%$, and the position angle of the polarization vectors (θ, counted from North to East) is -23°. Both quantities are very stable across the maser (Fig. 2, left-lower panel).

https://doi.org/10.1017/S1743921312006679 Published online by Cambridge University Press

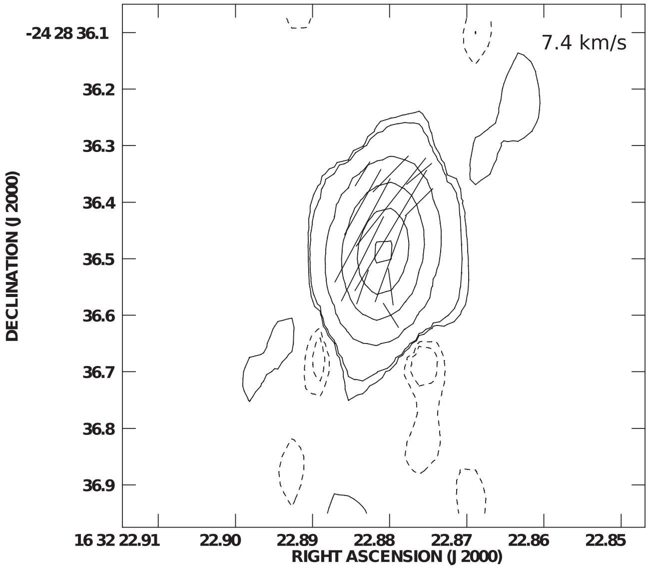

Figure 3. Distribution of H_2O linear polarization vectors in the brightest emission channel. Contours are -50, -30, 30, 50, 500, 3×10^3, 1×10^4, 2×10^4 $\times 8$ mJy beam^{-1}. Only polarization vectors whose $P > 1\%$ are plotted.

The line profile of the circular polarization (Stokes V) has the characteristic S-shape (Fig. 2, right-lower panel). It is proportional to the first derivative of the Stokes I spectrum and the LOS component of the magnetic field. The fraction of circular polarization, calculated as $(V_{max} - V_{min})/I_{max}$, is 0.45% for the brightest component. The remaining maser featuers show only residual Zeeman profiles with amplitudes at the rms level.

3. The B-field in I16293

From the Zeeman splitting formalism, the magnetic field strength can be correlated to the fraction of circular polarization P_V by (Fiebig & Guesten, 1989)

$$B \cos\theta = \frac{P_V \times \Delta V_I}{2 \times A_{F-F'}}, \tag{3.1}$$

where ΔV_I is the $FWHM$ of the total power spectrum and $A_{F-F'}$ is a coefficient which depends on the maser rotational levels F and F', the intrisic thermal linewidth $\Delta\nu_{th}$ and the maser saturation degree. The angle θ is the angle between the magnetic field and the maser propagation direction. Assuming that $A_{F-F'}$ ranges from 0.012 to 0.018 in order to be consistent with models and observations (Nedoluha & Watson 1992; Vlemmings *et al.* 2002), and a linewidth of 0.75 km s^{-1}, which is more realistic for resolved maser lines, the field strength is estimated to range between -94 and -141 mG, pointing towards the observer. Given that the linear polarization fraction is about 3%, this maser is likely unsaturated and the field strength determination is a fair approximation.

Fig. 3 shows the linear polarization vectors at the brightest channel. The direction of the plane-of-sky (POS) component of the magnetic field can be either perpendicular or parallel to the polarization vectors. However, since that our line is a blend of features spatially unresolved, we are unable to solve for this degeneracy, which depends on the maser saturation level and θ for each feature. Nevertheless, we can at least claim that the POS field topology is quite ordered in both cases, i. e., it would remain ordered when rotated by 90°.

4. Shock properties

The observed maser emission is excited in zones of compressed gas produced by shocks between the outflows and the ambient gas. In an ionized medium, shocks compress the gas and the magnetic field by a factor m_A, where $m_A = v_S/v_A$. While m_A is the so called Afvénic Mach number, v_S and v_A are the shock velocity and the Alfvén speed, respectively. Given that $v_A \propto B_0(n)^{-1/2}$ (where B_0 is the preshock magnetic field), the preshock density can be estimated by (Kaufman & Neufeld 1996)

$$n_0 = 1.6 \times 10^6 \left(\frac{B_s}{\mathrm{mG}}\right)^2 \left(\frac{v_S}{\mathrm{kms}^{-1}}\right)^2 \mathrm{cm}^{-3}, \tag{4.1}$$

where B_s is the magnetic field in the shocked region, calculated in §3. Using the shock velocities modeled by Ristorcelli *et al.*(2005), the preshock density is estimated as $\sim 1 \times 10^8$ cm^{-3}, consistent with typical preshock densities where water masers will be eventually pumped. Moreover, for such densities, the magnetic pressure ($B_s^2/8\pi$) is similar or higher than the shock ram pressure ($\rho_0 v_S$), and the outflow evolution is magnetically controlled.

Assuming flux-freezing of the well stablished magnetic field morphology reported by Rao *et al.* (2009), who estimated a POS field strength of 4.5 mG at densities of 5×10^7 cm^{-3} for I16293, the compression of this ordered field implies that

$$\frac{B_{Rao}}{n_{Rao}} = \frac{B_s}{n_s} \rightarrow n_s = 1.3 \times 10^9 \mathrm{cm}^{-3}, \tag{4.2}$$

which is expected for effective maser pumping.

5. Conclusions

We report spectro-polarimetric VLA observations of water masers toward I16293. The strong, but unresolved spatially emission is excited in zones of compressed gas where a mean LOS magnetic field strength of 113 mG is estimated. The postshock densities are consistent with the physical conditions for H_2O maser pumping, and the dynamical evolution of the outflow is likely regulated by the magnetic field.

References

Chandler, C. J., Brogan, C. L., Shirley, Y. L., & Loinard, L. 2005, *ApJ*, 632, 371
Claussen, M. J., Wilking, B. A., Benson, P. J., *et al.* 1996, *ApJS*, 106, 111
Elitzur, M., Hollenbach, D. J., & McKee, C. F. 1989, *ApJ*, 346, 983
Fiebig, D. & Guesten, R. 1989, *A&A*, 214, 333
Furuya, R. S., Kitamura, Y., Wootten, A., Claussen, M. J., & Kawabe, R. 2003, *ApJS*, 144, 71
Goodman, A. A., Jones, T. J., Lada, E. A., & Myers, P. C. 1995, *ApJ*, 448, 748
Imai, H., Nakashima, K., Bushimata, T., *et al.* 2007, *PASJ*, 59, 1107
Jørgensen, J. K., Bourke, T. L., Nguyen Luong, Q., & Takakuwa, S. 2011, *A&A*, 534, A100
Kaufman, M. J. & Neufeld, D. A. 1996, *ApJ*, 456, 250
Lazarian, A., Goodman, A. A., & Myers, P. C. 1997, *ApJ*, 490, 273
Nedoluha, G. E. & Watson, W. D. 1992, *ApJ*, 384, 185
Rao, R., Girart, J. M., Marrone, D. P., Lai, S.-P., & Schnee, S. 2009, *ApJ*, 707, 921
Ristorcelli, I., Falgarone, E., Schöier, F., *et al.* 2005, in: D. C. Lis, G. A. Blake & E. Herbst (eds.), *Astrochemistry: Recent Successes and Current Challenges*, Proc. IAU Symposium No. 231, p. 227
Vlemmings, W. H. T., Diamond, P. J., & van Langevelde, H. J. 2002, *A&A*, 394, 589
Vlemmings, W. H. T., Diamond, P. J., van Langevelde, H. J., & Torrelles, J. M. 2006, *A&A*, 448, 597